

Tubular Morphology of Mesoporous Silica MCM-41

Hong-Ping Lin^a (), Jyun-Hwei Hwang^b (),
Chung-Yuan Mou^{b,c,*} () and Chih-Yuan Tang^d ()

^a*Institute of Atomic and Molecular Sciences, Academia Sinica, P. O. Box 23-166, Taipei, Taiwan 106*

^b*Department of Chemistry, National Taiwan University, Taipei, Taiwan 106*

^c*Center of Condensed Matter, National Taiwan University, Taipei, Taiwan 106*

^d*Department of Zoology, National Taiwan University, Taipei, Taiwan 106*

We investigated detailed conditions for synthesizing the tubular form of MCM-41 mesoporous aluminosilicate. The method is the delayed neutralization method in which the rate of neutralization is one of the controlling factors. Rapid neutralization results in the particulate form while gradual neutralization leads to tubules. It is found that the tubule morphology has several sub-categories. There are thick-walled, thin-walled hollow tubular MCM-41 and solid core tubules. There are void structures in the channel framework that makes the nanochannels to be effectively interconnected.

INTRODUCTION

Recently, we reported that several micron-sized hierarchical structures, i.e. tubules-within-tubule (TWT)¹ and hollow pillared spheres (HPS),² could be successfully synthesized through soft and bendable intermediate of surfactant/silicate mesophase at the high alkalinity condition by careful control of the rate of acidification and the synthetic components. The MCM-41 nano-channels form the wall of these micrometer-sized hierarchical structures. Thus, the preparation of mesoporous aluminosilicate materials was elevated to a newly exciting level by having at least two length scales, namely, micro- and nano-meters.³ The ability to control structures in both length scales will have crucial impacts on catalysts, biomineralization, and design of the nanomaterials. In previous works that reported hierarchical order, the micron-scale structure is mostly generated by a separate mold, for example, by microemulsion⁴ or bacteria,⁵ as a template for growing the nanostructure. In contrast, our process involve a "liquid crystal phase transformation" mechanism.^{1,2} This then opens up a new approach to the design of hierarchical orders in inorganic nanomaterials, for many other complex orders can be achieved in complex liquid crystalline phases and modern theories of complex fluids⁶ have developed to the extent that it can help us to understand the associated phase changes.

In our previous reports,¹ we found that an ordered mesoporous molecular sieve MCM-41 with the tubules-within-a-tubule (TWT) hierarchical structure could be successfully synthesized in a highly alkaline condition by careful control of the surfactant-water content and the silica condensation rate. Liquid crystal phase transformation under a gradual neu-

tralization process, was proposed for the formation of the hierarchically ordered structure of C₁₆TMAB-aluminosilicate system.

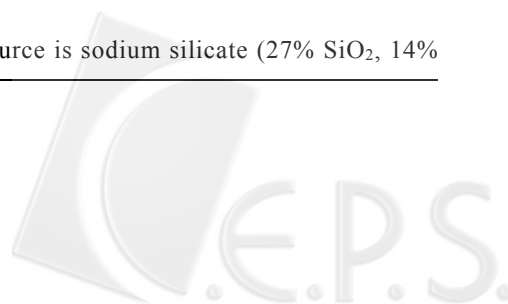
Subsequently, we found that this special tubular form of MCM-41 has a peculiar 3D pore system.⁷ This is due to many voids situated between the channels which effectively make the channels inter-connected as a three-dimensional network, and hence, inter-channel diffusion is possible. We demonstrated its advantage as a support in ethylbenzene dehydrogenation as the probe reaction.⁷ The tubular MCM-41 was shown to have higher catalytic activity when used as a catalyst support for ethylbenzene dehydrogenation.⁷ The enhanced activity in different morphology was attributed to the interconnection of the channels through voids in the framework.

Because the microtubular morphology of MCM-41 products is unusual in its facile transport, the details of this new morphology need to be examined carefully. In this paper, crucial factors, which alter the formation of MCM-41 materials in tubular structures are investigated in greater detail. It is found that the TWT structure actually encompasses many different tubular forms indicating variations in the micron-scale structures. And the void defects also vary. We report in these paper different forms of tubular MCM-41 from various synthetic conditions, which will be useful for the employment of TWT MCM-41 either in catalysis support or in adsorption.

EXPERIMENTAL

Materials

The silica source is sodium silicate (27% SiO₂, 14%



NaOH) from Aldrich, and the source of aluminum is sodium aluminate (AlNaO_2) from Riedel-de Haën. The alkyltrimethylammonium halides ($\text{C}_n\text{H}_{2n+1}(\text{CH}_3)_3\text{NX}$ ($n = 10-16$, C_nTMAX , $\text{X} = \text{Cl}$ or Br); Cetylpyridinium chloride ($\text{C}_{16}\text{H}_{33}\text{C}_5\text{H}_5\text{NCl}$) used as the surfactant templates are purchased from Tokyo Chemical Industry, Acrôs, Aldrich. The 1-alkanols (C_mOH) are from Merck. Sulfuric acid (H_2SO_4 ; 96%) is from Merck. All of these materials were used directly without further purification.

Synthesis

The typical synthetic procedure for preparing the pure silica and aluminosilicate MCM-41 mesoporous materials is based on the delayed-neutralization process reported in one of our previous papers.⁸ The "fast neutralization" procedure was used for preparing the microparticle-shaped mesoporous MCM-41 samples, and the "gradual neutralization" procedure was performed to synthesize the TWT hierarchical structure. The molar composition of the resultant gel is: 1.0 C_nTMAX : 2.10 SiO_2 : (0-0.21) AlNaO_2 : (1.63-1.20) NaOH : (0-1.0) C_mOH : (0.67-0.40) H_2SO_4 : (50-500) H_2O . The resulted gel mixture hydrothermally reacted at 100 °C for 48 h in a static autoclave. The as-synthesized product was recovered by filtration and washing process with a variety of deionized water, then calcined at 560 or 580 °C in air for 6 h for removing the templates.

Characterization

The powder x-ray diffraction (XRD) patterns of the as-synthesized and calcined samples were collected on a Scintag X1 diffractometer using $\text{Cu K}\alpha$ ($\lambda = 0.154$ nm) radiation. N_2 adsorption-desorption isotherms of the calcined samples were obtained on a Micromeritics ASAP 2010 system at 77 K with samples outgassed at 250 °C under 10^{-3} torr for at least 3 h. Bulk mesoporous materials for TEM characterization were embedded in Spur resin and cured at 60 °C overnight. Ultrathin sections (approximately 30-50 nm) were cut from the embedded specimen using a diamond knife at room temperature. Sections were picked up on copper grids. The transmission electron micrographs (TEM) were recorded on a Hitachi H-7100 micrometer operated at 75-100 keV. Scanning electron microscopy (SEM) was performed on a Hitachi S-800 operated at an accelerating voltage of 20 keV.

RESULTS AND DISCUSSION

In this section, we present the results of morphology investigation under various synthetic conditions. It has been known that the condition for making tubular MCM-41 is much

more restricted than the normal particulate form.^{1,9} There are many factors that need to be carefully controlled. These are the water/surfactant ratio, surfactant chain length, counterion, and the rate of acidification of the gel solution. We will examine them individually.

Let us first examine the effect of the rate of neutralization. In the delayed-neutralization process, the surfactant/silicate solution is initially at high alkaline condition, $\text{pH} > 13$. One has to add acid to start the formation of oligomer of silicates. Only then can the silicates begin to exchange for the counterions of the rod micelles which finally lead to the formation of the hexagonal phase.¹⁰ It turns out the rate of neutralization is crucial for the formation of tubular MCM-41.¹¹

Fig. 1 shows the framework structure and morphology of the MCM-41, from CTAB and sodium silicates, under rapid neutralization Process. Only the sub-micron particulate form of MCM-41 is observed (Fig. 1A). TEM (Fig. 1B, C) micrograph indicates the nanostructure of the hexagonal framework is well-ordered containing little defects. Fig. 1D illustrates schematically the well-ordering of the hexagonal phase.

However, when one decreases the pH value of initial

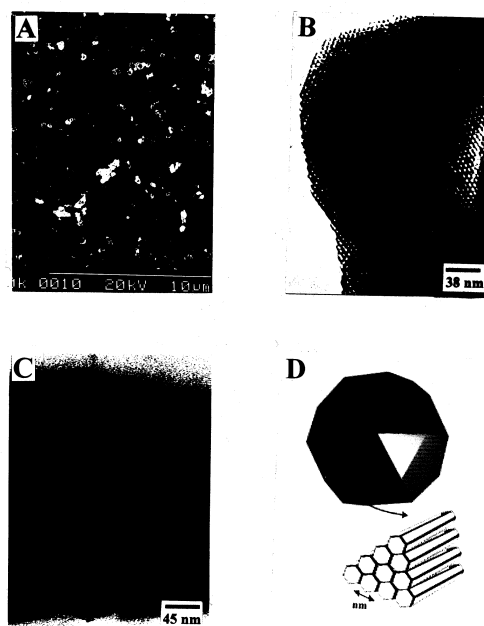


Fig. 1. The SEM and TEM micrographs of the microparticle shaped mesoporous sample synthesized from the compositions of 1 C_{16}TMAX : 2.10 SiO_2 : 0.68 NaOH : 0.29 H_2SO_4 : 165 H_2O by a fast neutralization process. A. SEM micrograph; B. TEM micrograph viewed along the channels direction; C. TEM micrograph viewed perpendicular to the channels direction; D. a schematic diagram of the mesostructures of the microparticle.

surfactant/silicate very slowly by gradual neutralization, the morphology of MCM-41 becomes predominately tubular. The tubular form is formed in the room temperature stage and it survives the subsequent hydrothermal treatment and calcination. Fig. 2A shows the morphology of tubular MCM-41; the lengths of the tubules are more than 100 nm. Fig. 2B shows that the tubules are hollow. It should be noted that the samples shown in Fig. 1 and Fig. 2 start from almost exactly the same gel composition. The rate of neutralization is the only different factor.

Next, we add aluminum source NaAlO_2 to the initial gel, while the surfactant and silicates are still the same. Here the water contents also increased somewhat in order to keep producing the tubular form of the aluminosilicate MCM-41. Fig. 3A shows the SEM micrograph of the calcined product. The diameters of the tubules are rather uniform at about 0.5 micrometer. The yield is rather high at about 95%. This is the result of phase transformation rather than chemical kinetic control. Fig. 3C, however, shows that the tubules are solid inside (not hollow), but containing many voids.

The TEM picture in Fig. 3D and E again confirm that the tubules do not have the central end-to-end big channel as in the hollow TWT. Instead, one finds many small voids dispersed among the nanochannels. Fig. 3F shows the schematic drawing of the defects in the tubule.

On the other hand, when one used the surfactant C_{16}PyCl , the water content needs to increase to a higher value to form tubular MCM-41. In this case, one finds a hollow tubular MCM-41 with a much bigger central cavity. Fig. 4 and B show the morphology of the materials; the yield is again rather high. On closer examination by TEM (Fig. 4C), one sees the tubules are rather empty inside. Fig. 4D shows an ultra-thin section across the tubule with a hollow tubule with a very thin wall, which is rather transparent under a TEM electronic microscope. The TEM micrograph in Fig. 4E shows the external

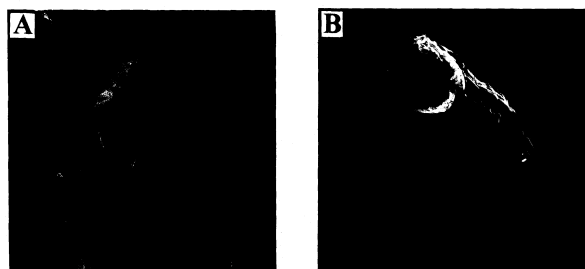


Fig. 2. The SEM micrographs of the microparticle-shaped mesoporous sample synthesized from the compositions of 1 C_{16}TMAB : 2.10 SiO_2 : 0.68 NaOH : 0.29 H_2SO_4 : 163 H_2O by a gradual neutralization process. A. SEM micrograph; B. SEM of a hollow TWT structure.

wall is rather defective.

To successfully synthesize the tubular MCM-41, the length of the surfactant chain and the composition need to be in a rather narrow range. Another example is by using the mixed surfactant C_{18}TMAB and C_{10}TMAB in the synthetic gel. The change of octadecyltrimethylammonium bromide (C_{18}TMAB)/decyltrimethylammonium bromide (C_{10}TMAB) ratio gives different micrometer-scaled structures. Given an optimum neutralization rate, the morphology of MCM-41 at both $[\text{C}_{18}\text{TMAB}]/[\text{C}_{10}\text{TMAB}] = 1$ and $[\text{C}_{18}\text{TMAB}]/[\text{C}_{10}\text{TMAB}] = 5-8$ is a small particle, also while at $[\text{C}_{18}\text{TMAB}]/[\text{C}_{10}\text{TMAB}] = 3$, the system gives TWT structure. We found

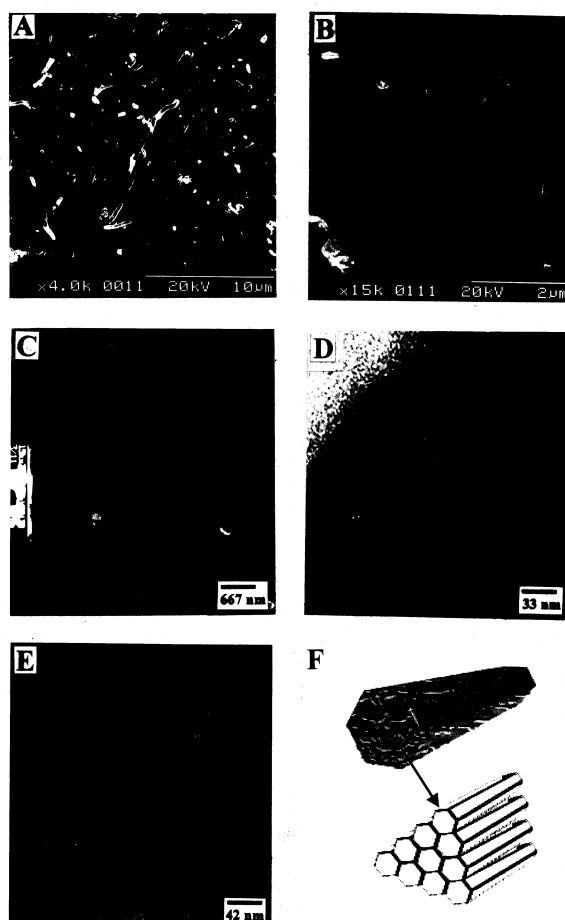


Fig. 3. The SEM and TEM micrographs of the microparticle-shaped mesoporous sample synthesized from the compositions of 1 C_{16}TMAB : 2.10 SiO_2 : 0.68 NaOH : 0.29 H_2SO_4 : 178 H_2O by a gradual neutralization process. A. SEM micrograph; B. larger-magnification SEM; C. microtome TEM micrograph; D. microtome TEM micrograph viewed along the channels direction; E. microtome TEM micrograph viewed perpendicular to the channels direction; F. a schematic diagram of the mesostructures of the TWT hierarchical structure.

that the optimum average chain length for preparing TWT structure is 15 ~ 16 for the mixed C_n TMABr system and 16 ~ 17 for the mixed C_n TMACl system.⁹ The underlying determining factor is the average hydrophobicity of the surfactants employed.⁹

For shorter chain surfactants, adding a cosurfactant, medium chain alcohol, can also help the formation of better structured MCM-41. We also tried its use in helping the formation of tubular MCM-41. Fig. 5 shows the SEM micrographs for C_n TMAX ($n < 16$) with the use of the co-surfactant alcohol. Without alcohols, these surfactants could not form tu-

bular morphology at all conditions we tried. The SEM of the MCM-41 materials synthesized from C_{12} TMAB- C_4 OH-silicate with different water content shows that the tubular morphology could be formed only in a suitable range. At lower water content, the sample is only in micro-particle even with changing the C_m OH concentration. When increasing the water content, the tubular morphology can be synthesized at a proper range of the C_m OH/surfactant ratio.¹² All of these samples have well-arranged hexagonal MCM-41 structure. To adjust the proper hydrophobicity for tubular morphology, butanol is proper for matching C_{14} TMA+ surfactant (Fig. 5B and C) and hexanol is better for C_{12} TMA+ (Fig. 5D).

The physical characterization of these tubular MCM-41 materials is also performed using XRD. Fig. 6A shows the XRD patterns of the calcined MCM-41 samples synthesized from C_{16} TMABr-silicate by using the delayed neutralization process. In Fig. 6, sample I. II. III. IV. V. correspond to materials images shown in Figs. 1, 3, 4, 5C and 5D, respectively. There exist at least 4 sharp XRD peaks for all these samples, indicating a well-ordered hexagonal structure of MCM-41. These results are consistent with previously reported results that the incorporation of aluminum into silica framework do

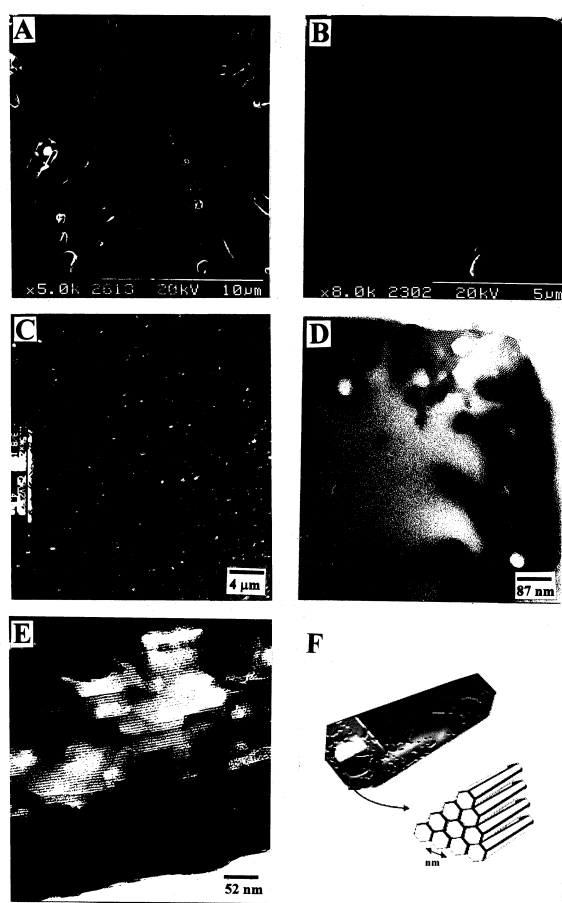


Fig. 4. The SEM and TEM micrographs of the micro-particle-shaped mesoporous sample synthesized from the compositions of 1 C_{16} PyCl : 2.10 SiO_2 : 0.68 NaOH : 0.29 H_2SO_4 : 206 H_2O by a gradual neutralization process. A. SEM micrograph; B. larger-magnification SEM; C. microtome TEM micrograph; D. microtome TEM micrograph viewed along the channels direction; E. microtome TEM micrograph viewed perpendicular to the channels direction; F. a schematic diagram of the mesostructures of the TWT hierarchical structure.

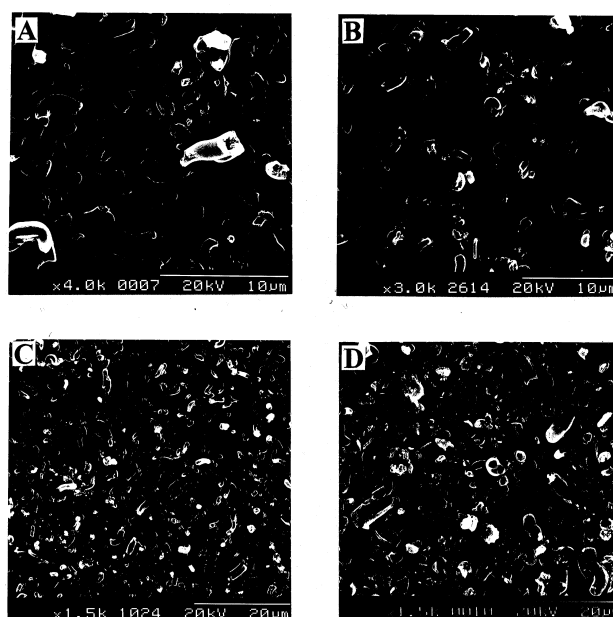


Fig. 5. The SEM micrographs of the mesoporous sample with hollow TWT structure prepared from the compositions of 1 C_n TMAX : 2.10 SiO_2 : 0.68 NaOH : 0.29 H_2SO_4 : (0-1.0) C_m OH : (200-300) H_2O by a gradual neutralization process. A. SEM micrograph of 1 C_{16} TMACl; B. SEM micrograph of 1 C_{14} TMAB : 0.80 C_4 OH; C. SEM micrograph of 1 C_{14} TMACl : 0.96 C_4 OH; D. SEM micrograph of 1 C_{12} TMAB : 0.35 C_6 OH.

not have a significant effect on the ordering of meso-structure. However, examining the N_2 adsorption-desorption isotherms of these samples (Fig. 6B), one can clearly see that a sharp inflection which is common to all these samples exists at $p/p_0 =$

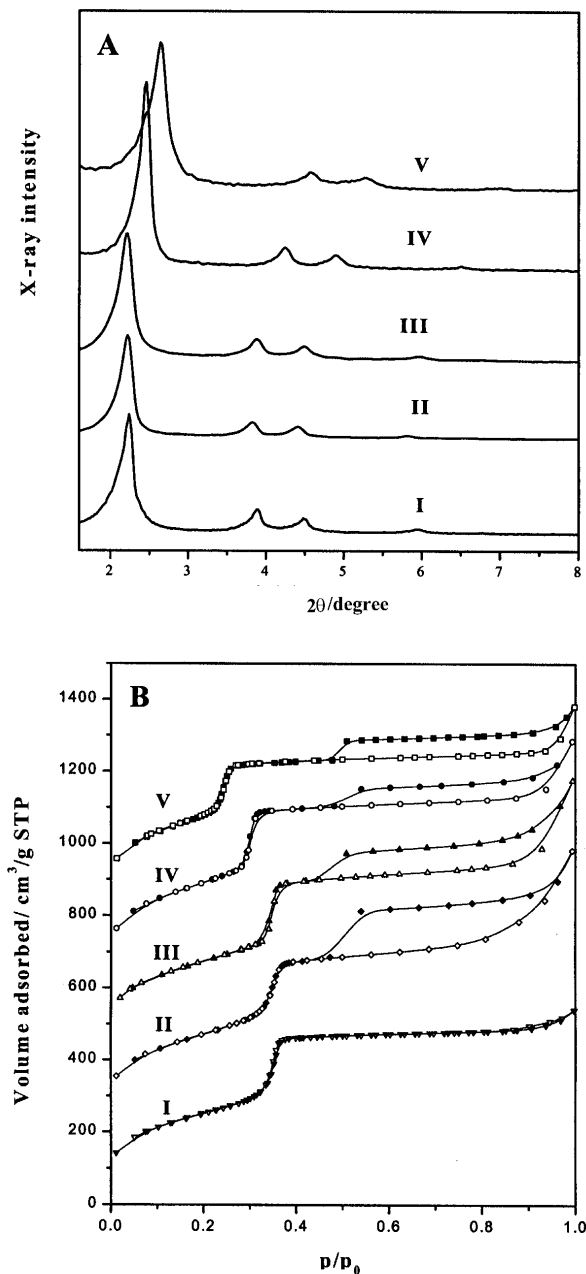


Fig. 6. The XRD patterns and N_2 adsorption-desorption isotherms of the mesoporous sample in Fig. 1-4. A. XRD patterns; B. N_2 adsorption-desorption isotherms. I. sample of Fig. 1; II. sample of Fig. 2; III. sample of Fig. 3; IV. Sample of Fig. 4C; V. sample of Fig. 4D. In Fig. 6B, the amount adsorbed for sample II, III, IV, V was increased by 200, 400, 600, 800 cm^3/g STP, respectively.

0.32. This inflection is typical of a capillary condensation process and the p/p_0 value corresponds to a pore size of about 2.6 nm (calculated from the BJH method), except for a smaller pore size for sample V. The pore size distribution of these samples is also narrow, and the full width at half maximum (FWHM) is only about 0.15 nm. From the corresponding TEM micrographs, we found that those sample (particulate) showing little structural defects also give no or little adsorption hysteresis. However, all the tubular samples (II to V) have an additional and uncommon type-H3 hysteresis loop (de Boer's classification) at p/p_0 between 0.5 and 1. Here, we define the size of hysteresis loop in the isotherm as the difference in N_2 adsorption volume between the desorption and adsorption branches in the aforementioned range. The size of the hysteresis loop is the highest for sample II in which are also observed the most abundant voids. The existence of such a type-H3 hysteresis loop can be attributed to the formation of void defects in the MCM-41 hexagonal matrix, in which the sharp drop of isotherm in the desorption hysteresis curve is due to pore-blocking of those voids.

CONCLUSIONS

In this paper, we have examined the different tubular morphologies made from quaternary ammonium surfactant, co-surfactant, and silicates. The central hollow channel of the micron-size tubules could have various sizes or do not exist at all. Regardless of these differences, all the tubular MCM-41 materials possess void defects in the framework. This leads to an effectively interconnected 3D nanochannel system. This void defects promote the transport of adsorbents or reagents in applications.

We also found that although the surfactant hydrophobicity is rather restricted for the formation of tubules, one could use co-surfactant (alcohol) or adjusting water content to promote the formation of tubules. This makes possible some limited room of adjustment to form tubular MCM-41 with different pore size.

ACKNOWLEDGEMENTS

This research was supported by the China Petroleum Co. and the National Science Council of Taiwan (NSC 88-2113-M-002-027).

Received May 30, 2000.



Key Words

MCM-41; Tubular; Morphology; Synthesis.

REFERENCES

1. (a) Lin, H. P.; Mou, C. Y. *Science* **1996**, 273, 765. (b) Lin, H. P.; Cheng, S.; Mou, C. Y. *Chem. Mater.* **1998**, 10, 581.
2. Lin, H. P.; Cheng, Y. R.; Mou, C. Y. *Chem. Mater.* **1998**, 10, 3772.
3. Tanev, P. T.; Liang, Y.; Pinnavaia, T. J. *J. Am. Chem. Soc.* **1997**, 119, 8616.
4. Schacht, S.; Hou, Q.; Voigt-Martin, I. G.; Stucky, G. D.; Schüth, F. *Science* **1996**, 273, 768.
5. Davis, S. A.; Burkett, S. L.; Mendelson, N. H.; Mann, S. *Nature* **1997**, 385, 420.
6. Porte, G. *J. Phys. Condensed Mater.* **1997**, 4, 8649.
7. Wong, S.-T.; Lin, H. P.; Mou, C.-Y. *Applied Catalyst.* **2000**, 198, 103.
8. Lin, H. P.; Cheng, S.; Mou, C. Y. *Microporous Mater.* **1996**, 10, 111.
9. Cheng, Y.-R.; Lin, H. P.; Mou, C. Y. *Phys. Chem. Chem. Phys.* **1999**, 1, 5051.
10. Huo, S.; Margolese, I.; Ciesla, U.; Demuth, D. G.; Feng, P.; Gier, D. E.; Sieger, P.; Chmelka, B. F.; Schuth, F.; Stucky, G. D. *Chem. Mater.* **1994**, 6, 176.
11. Lin, T.-R.; Wan, B.-Z.; Lin, H. P.; Mou, C.-Y. *The Materials Research Society* **1999**, Vol II, 931.
12. Lin, H. P.; Cheng, Y.-R.; Liu, S.-B.; Mou, C.-Y. *J. Materials Chem.* **1999**, 1197.

